Tunneling spectroscopy as a probe of c-axis variation of $d_{a^2-b^2}$-wave order parameter

P. Pairor*
School of Physics, Institute of Science, Suranaree University of Technology, Nakhon Ratchasima, 30000 Thailand
(Received 5 July 2005; revised manuscript received 16 September 2005; published 29 November 2005)

The effect of variation along c axis of the $d_{a^2-b^2}$-wave order parameter on tunneling spectra of normal metal-superconductor junctions with various orientations is theoretically investigated. It is found that the zero-bias conductance peak is virtually unaffected by this variation. In particular, the variation causes a small decrease in the width and does not change the height. On the contrary, the coherence peak of the conductance spectra is affected by this variation. The peak gets wider as the c-axis variation of the order parameter is larger. The width of the coherence peak in tunneling spectrum can thus be used to measure the c-axis variation of the order parameter.

DOI: 10.1103/PhysRevB.72.174519 PACS number(s): 74.20.−z, 74.25.Jb

I. INTRODUCTION

Different characteristics of superconducting order parameters lead to a variety of features that can be observed in normal metal-superconductor tunneling conductance spectra. For instance, due to a large number of states at the energy gap, a coherence peak occurs at the corresponding applied voltage in the tunneling spectra. It is well known that the peak position provides accurate measurement for the magnitude of the superconducting gap.[1–3] For unconventional superconductors, tunneling spectroscopy is a valuable tool for obtaining the gap symmetry. If there is a sign change in the order parameter, then a zero-bias conductance peak (ZBCP) in the tunneling spectrum is predicted.[4–8] By varying the tunneling junction orientation with respect to the superconductor crystal axes, the observation of the zero-bias conductance peak can be used to locate sign changes in the gap function and thus determine its symmetry. There have been many tunneling experiments that revealed zero-bias conductance peaks in the tunneling spectra of copper-oxide-based superconductors (see, for example, Refs. 9–21). The existence of this peak in part has provided supporting evidence for $d_{a^2-b^2}$-wave symmetry of the order parameter in these materials.

The tunneling spectra can also potentially be used to measure the variation of the gap magnitude of anisotropic superconductors. The value of the energy gap along the direction perpendicular to the plane of a smooth junction can be obtained using the position of the coherence peak in the tunneling spectrum.[22,23] Such additional features occurring in the spectrum, and their variation with junction orientation, undoubtedly contain useful information about the gap function. An understanding of how various characteristics of the superconducting order parameter determine these features is needed to correctly extract this information from tunneling data. For this purpose, the effect that finite pairing interactions along the c axis of layered materials have on the tunneling spectra may be considered. For superconductors with two layers in a unit cell, the c-axis coupling between bilayers may be included. The effect of the bilayer coupling has been studied by many groups[24–28] and found to have many interesting consequences, such as a contribution to the order parameter anisotropy[25] and the splitting of the coherence peak in the density of states.[27,28] In materials with only one layer per unit cell, one may include the interaction between layers of adjacent unit cells.

The hopping of quasiparticles between layers of adjacent unit cells reveals itself as a nonvanishing k_z dispersion relation of the band structure, while the pairing interaction between the layers does so as a k_z variation of the order parameter. The inclusion of the former leads to irreducible broadening of line shape in angle-resolved photoemission spectroscopy[29] and enhances the splitting of the two bands with two copper-oxide planes per unit cell.[27] There has not yet been much study of the importance of the c-axis variation of the order parameter. It was shown that the nonzero interaction between the layers of adjacent unit cells can cause the order parameter to vary along k_z as $\Delta(\phi,k_z)=[\Delta_0+\Delta_1\cos(k_z c)]\cos 2\phi$,[30–32] where Δ_0 and Δ_1 are the intralayer and interlayer pairing order parameter respectively (for weak interactions between the planes $\Delta_1 \ll \Delta_0$), ϕ is the direction in the ab plane with respect to the a axis, k_z is the z component of the wave vector, and c is the lattice constant along the c axis. This article is a theoretical study of the effect of such interlayer interactions on tunneling spectra. A principle goal is to look into this effect on both ab-plane and c-axis tunneling spectroscopy of quasi-two-dimensional $d_{a^2-b^2}$-wave superconductors. As will be shown later, this variation of the order parameter mainly affects the width of the coherence peak of the tunneling spectrum of both types of the junctions. A more rigorous calculation is presented later in the article, but here a simple explanation for the qualitative behavior will be given.

The conductance spectra of {100} and {001} junctions in the tunneling limit are similar to the density of states of the superconductor. By considering the expansion of the energy dispersion relation, one can identify energy values corresponding to minima, maxima, and saddle points, i.e., Van Hove singularities (see, for example, Ref. 33, pp. 69–75). In the case where $\Delta(\phi,k_z)=[\Delta_0+\Delta_1\cos(k_z c)]\cos 2\phi$, consider energies $E_k=\sqrt{\xi_k^2+|\Delta(\phi,k_z)|^2}$ close to $\Delta(\phi=0,k_z=0)=\Delta_0+\Delta_1$ and to $\Delta(\phi=0,k_z=\pm\pi/c)=\Delta_0-\Delta_1$, which respectively are the maximum and minimum values of the gap function along the ac plane. The energy E_k can be written as an expansion around $k_\pm$, where $E_{k_\pm}=\Delta_0\pm\Delta_1$, as

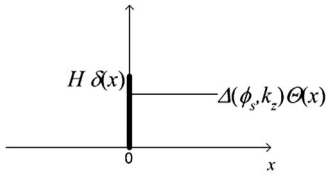

FIG. 1. The normal metal-superconductor junction is represented by an infinite system. The normal metal and the superconductor occupy the $x<0$ region and the $x>0$ region, respectively. The insulating layer is represented by a delta function of height H. The gap function is taken to be $d_{a^2-b^2}$-wave with variation along k_z, $\Delta(\phi,k_z)=[\Delta_0+\Delta_1\cos(k_z c)]\cos 2\phi$ as described in the text.

$$E_k \approx (\Delta_0 \pm \Delta_1) + \beta_1 k_\perp^2 + \beta_2 k_\parallel^2 + \beta_3 k_z^2, \tag{1}$$

where $k_\perp$ and $k_\parallel$, which are measured from the Fermi surface, are the components perpendicular and parallel to the Fermi surface respectively, $\beta_1=\frac{1}{2}(\hbar v_F)^2/(\Delta_0\pm\Delta_1)$, $\beta_2=-(\Delta_0\pm\Delta_1)/k_F^2$, and $\beta_3=\mp\frac{1}{2}\Delta_1 c^2/\Delta_0$. In the case of interest here, $\Delta_1 \ll \Delta_0$, so $\beta_1>0$ and $\beta_2<0$. That is, $k_\pm$ are saddle points. These saddle points give rise to kinks in the density of states at $E_{k_\pm}=\Delta_0\pm\Delta_1$. The nonzero Δ_1 should therefore lead to a blunt peak with the width of $2\Delta_1$ in the density of states. Here, the definition of the width is the distance in energy between the two discontinuities of the slopes in the density of states.

The c-axis variation of the order parameter does not have much effect on the zero-bias conductance peak. This aspect will be discussed in more detail in Section III. In the next section, a brief explanation of the model and method used in the calculation will be given. The conductance spectra of ab-plane and c-axis junctions will be shown and discussed in Sec. III. Section IV is the conclusion of this article.

II. MODEL AND ASSUMPTIONS

This article follows a method, first introduced in Ref. 34 to calculate the transmission probabilities for thermal and electrical currents of a normal metal-superconductor junction and, as later used in Ref. 35 to study the transition from the metallic to the tunneling regimes for a single junction. In this approach, a normal metal-superconductor junction is modeled as an infinite system, the left half of which is a normal metal and the right half of which is a superconductor, as shown in Fig. 1. The insulating barrier is represented by a delta function potential of strength H. The order parameter is taken to be

$$\Delta(\phi,k_z) = [\Delta_0 + \Delta_1\cos(k_z c)]\cos 2\phi, \tag{2}$$

where Δ_0 and Δ_1 are the intralayer and interlayer pairing order parameter respectively, ϕ is the direction in the ab plane with respect to the a axis, k_z is the z component of the wave vector, and c is the lattice constant along the c axis. For ab-plane tunneling junctions, the interface normal vector lies somewhere in the ab plane, and for c-axis tunneling junctions the interface normal is parallel to the c axis.

A continuous model is used to describe the electronic structures of both normal metal and superconductor. That is, the Bogoliubov-de Gennes equations of the excitations of the system are

$$\begin{bmatrix} \hat{O}_p + H\delta(x) - \mu & \Delta(\phi_s,k_z)\Theta(x) \\ \Delta^*(\phi_s,k_z)\Theta(x) & -(\hat{O}_p + H\delta(x) - \mu) \end{bmatrix} U(\vec{r}) = EU(\vec{r}), \tag{3}$$

where μ is the chemical potential, $\Theta(x)$ is the Heaviside step function, and

$$\hat{O}_p = -\frac{\hbar^2}{2m_{ab}}\left(\frac{\partial^2}{\partial x^2}+\frac{\partial^2}{\partial y^2}\right) - \frac{\hbar^2}{2m_c}\frac{\partial^2}{\partial z^2}, \tag{4}$$

where

$$m_{ab} = \begin{cases} m, & x<0 \\ m_{ab}^s, & x>0 \end{cases} \tag{5}$$

and

$$m_z = \begin{cases} m, & x<0 \\ m_c^s, & x>0 \end{cases}. \tag{6}$$

In all cases, m_{ab}^s, the ab plane effective mass of a superconducting quasiparticle, is taken to be equal to m, the effective mass of an excitation in the normal metal. In the calculation related to ab-plane junctions, m_c^s, the c-axis effective mass of the superconductor, is set to be infinity for simplicity. In ab-plane tunneling spectra, the energy dispersion relation along k_z, or the finiteness of m_c^s, does not play an important role, because the currents across the junction are mainly from the states with velocities parallel to the plane. However, for the calculation related to c-axis tunneling, m_c^s is set to 100 m to account for the fact that there exists current across the c-axis junction and that the anisotropy between the ab plane and the c axis is at least of the order 100.[36–39] The two-component function $U(\vec{r})$ is

$$U(\vec{r}) = \begin{cases} U_N(\vec{r}), & x<0 \\ U_S(\vec{r}), & x>0 \end{cases}. \tag{7}$$

The matching conditions for the wave functions at the interface of ab-plane junctions are

$$U_N(x=0) = U_S(x=0) \equiv U_0, \tag{8}$$

$$ZU_0 = \frac{1+m/m_{ab}^s}{4k_F}\left(\left.\frac{\partial U_S}{\partial x}\right|_{0^+} - \left.\frac{\partial U_N}{\partial x}\right|_{0^-}\right), \tag{9}$$

where $Z=mH/(\hbar^2 k_F)$ and k_F is the magnitude of the Fermi wave vector of the superconductor. For c-axis tunneling junctions, the first condition remains the same, but in the second condition m_{ab}^s must be replaced with m_c^s.

Due to the translational symmetry along the plane of interface, for ab-plane junctions the two wave functions can be written as

$$U_N(\vec{r}) = U_N(x)e^{i(k_y y + k_z z)}, \tag{10}$$

$$U_S(\vec{r}) = U_S(x)e^{i(k_y y + k_z z)}, \tag{11}$$

where $U_N(x) = U_{N0}e^{iqx}$ and $U_S(x) = U_{S0}e^{ikx}$. In the case where the interface normal is parallel to c axis, the following replacements are needed: $x \to z$, $y \to x$, and $z \to y$.

The bulk excitation energies for the normal metal are

$$E(\vec{q}) = \pm \xi_q, \tag{12}$$

where the plus and minus signs are for electron and hole excitations respectively, and

$$\xi_q = \begin{cases} \dfrac{\hbar^2}{2m}(q^2 + q_y^2 + q_z^2) - \mu & (ab\text{-plane junctions}) \\ \dfrac{\hbar^2}{2m}(q^2 + q_x^2 + q_y^2) - \mu & (c\text{-axis junctions}). \end{cases} \tag{13}$$

For the superconductor,

$$E(\vec{k}) = \sqrt{\xi_k^2 + |\Delta(\phi, k_z)|^2}, \tag{14}$$

where

$$\xi_k = \begin{cases} \dfrac{\hbar^2}{2m_{ab}^s}(k^2 + k_y^2) + \dfrac{\hbar^2}{2m_c^s}k_z^2 - \mu & (ab\text{-plane junctions}). \\ \dfrac{\hbar^2}{2m_c^s}k^2 + \dfrac{\hbar^2}{2m_{ab}^s}(k_x^2 + k_y^2) - \mu & (c\text{-axis junctions}). \end{cases} \tag{15}$$

Note that for an ellipsoidal surface one can always find new coordinates k_x', k_y', k_z', in which it becomes spherical. That is, $k_x' = k_x\sqrt{m^*/m_{ab}^s} = k_F \cos\phi \sin\theta$, $k_y' = k_y\sqrt{m^*/m_{ab}^s} = k_F \sin\phi \sin\theta$, and $k_z' = k_z\sqrt{m^*/m_c^s} = k_F \cos\theta$, where m^*, k_F are adjustable parameters.

The amplitude of the excitations, U_{N0}, in the normal metal is $\binom{1}{0}$ for electrons and is $\binom{0}{1}$ for holes, whereas the amplitude of the excitations in the superconductor is

$$U_{S0} = \frac{1}{\sqrt{|E + \xi_k|^2 + |\Delta(\phi, k_z)|^2}} \begin{pmatrix} E + \xi_k \\ \Delta(\phi, k_z) \end{pmatrix}. \tag{16}$$

The wave function of each side is a linear combination of all the appropriate excitations of the same energy and the momentum that has the same component perpendicular to the interface normal. That is,

$$U_N(x) = \begin{pmatrix} 1 \\ 0 \end{pmatrix} e^{iq^+ x} + a\begin{pmatrix} 0 \\ 1 \end{pmatrix} e^{iq^- x} + b\begin{pmatrix} 1 \\ 0 \end{pmatrix} e^{-iq^+ x}, \tag{17}$$

$$U_S(x) = c\begin{pmatrix} u_{k^+} \\ v_{k^+} \end{pmatrix} e^{ik^+ x} + d\begin{pmatrix} u_{-k^-} \\ v_{-k^-} \end{pmatrix} e^{-ik^- x}, \tag{18}$$

where

$$q^\pm = \sqrt{2m(\mu \pm E)/\hbar^2 - q_y^2 - q_z^2},$$

$$k^\pm = \sqrt{2m[\mu \pm \sqrt{E^2 - \Delta^2(\phi, k_z)}]/\hbar^2 - k_y^2 - k_z^2}$$

are the parallel-to-the-interface-normal components of the normal and superconducting wave vectors, respectively, and

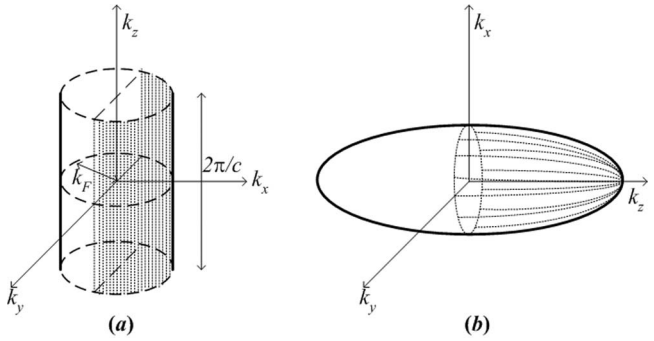

FIG. 2. The sketches of the Fermi surfaces of the layered superconductors used to calculate the conductance spectra of (a) ab-plane junctions and (b) c-axis junctions. For simplicity, a cylindrical Fermi surface is used for ab-plane junctions, whereas an ellipsoidal Fermi surface is used for c-axis junctions. The shadowed region of each surface indicates the states contributing to the current across the junction.

a, b, c, and d are the Andreev reflection, the normal reflection, the same-branched transmission, and the cross-branched transmission amplitudes, respectively. These amplitudes are obtained using the matching conditions in Eqs. (8) and (9).

Normally, the range of the energy E relevant to the tunneling experiments is of order meV whereas the Fermi energy is of order 0.1–1 eV. Therefore, the following approximations for $q^\pm$ and $k^\pm$ are applicable:

$$q^+ = q^- = \begin{cases} q_F \sin\theta_N \cos\phi_N & (ab\text{-plane junctions}) \\ q_F \cos\theta_N & (c\text{-axis junctions}) \end{cases} \tag{19}$$

$$k^+ = k^- = \begin{cases} k_F \cos\phi_S & (ab\text{-plane junctions}) \\ k_F\sqrt{\dfrac{m_c^S}{m^*}} \cos\theta_S & (c\text{-axis junctions}), \end{cases} \tag{20}$$

where q_F denotes the magnitude of the Fermi wave vector of the normal metal. Note that the different values for $k^\pm$ in ab-plane and c-axis junctions are due to different junction orientation and different Fermi surfaces. As already mentioned, without losing generality of the results, cylindrical Fermi surface can be used to calculate the conductance of ab-plane junctions (see Fig. 2). However, in case of c-axis junctions one needs to include the three dimensionality in the Fermi surface by taking m_c^s to be finite. Therefore, k_F, m^* in Eq. (20) are taken to be the parameters that satisfy $\hbar^2 k_F^2/(2m^*) = E_F^S$, the Fermi energy of the superconductor. Using the conservation of the momentum parallel to the surface, the relationships between the polar angles for ab-plane junctions are

$$q_F \sin\theta_N \sin\phi_N = k_F \sin\phi_S, \tag{21}$$

$$q_z = q_F \cos\theta_N = k_z. \tag{22}$$

Similarly, for c-axis junctions the relationships are

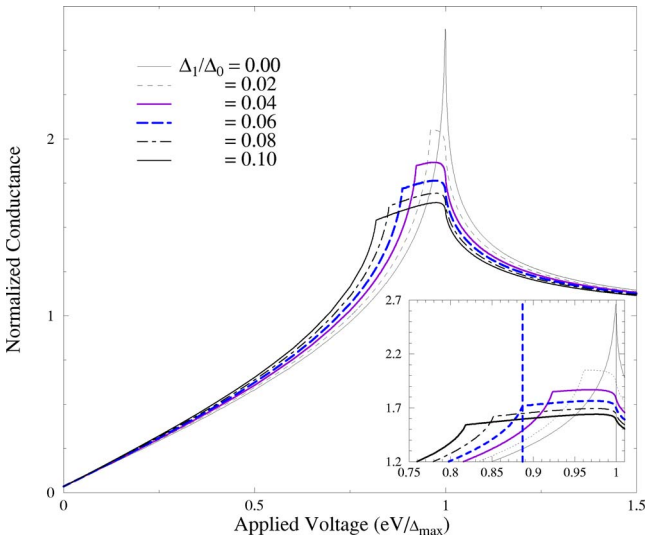

FIG. 3. (Color online) The conductance curves of {100} junctions for different values of Δ_1. The inset shows the detailed conductance curve around maximum gap, $\Delta_{max}=\Delta_0+\Delta_1$. The vertical solid line indicates the maximum gap and the dotted vertical line marks $\Delta_0-\Delta_1$, where $\Delta_1=0.06\Delta_0$ as an example.

$$q_F \sin\theta_N \sin\phi_N = k_F \sqrt{\frac{m_{ab}^s}{m^*}} \sin\theta_S \sin\phi_S, \tag{23}$$

$$q_F \sin\theta_N \cos\phi_N = k_F \sqrt{\frac{m_{ab}^s}{m^*}} \sin\theta_S \cos\phi_S. \tag{24}$$

By following the formalism in Ref. 35, one can obtain the expression for the current across the junction as a function of the applied voltage V as

$$I_{NS}(V) = \frac{e\Omega}{(2\pi)^3} \int d\vec{q}\, v_{q_x}[1 + A(\vec{q}) - B(\vec{q})] \times [f(E_q - eV) - f(E_q)], \tag{25}$$

where Ω is the volume, v_{q_x} is the component parallel to the interface normal vector of the group velocity of the incoming electron, $f(E)$ is the Fermi-Dirac distribution function, and $A=|a|^2(q^-/q^+)$, $B=|b|^2$ are the probabilities of Andreev and normal reflections, respectively.

The conductance of the ab-plane junction at zero temperature is then

$$G_{NS}^{ab}(V) = \frac{dI_{NS}^{ab}}{dV},$$

$$= \frac{2me^3\Omega}{(2\pi\hbar)^3} V \int d\phi_N \int d\theta_N \sin^2\theta_N \cos\phi_N \times [1 + A(V,\phi_N,\theta_N) - B(V,\phi_N,\theta_N)], \tag{26}$$

where Ω is the volume, and θ_N, ϕ_N are the angles in spherical coordinates for the normal metal. In the calculation, q_F is set to be $10k_F$, and $c=3a$, where a is the lattice constant along the a axis.

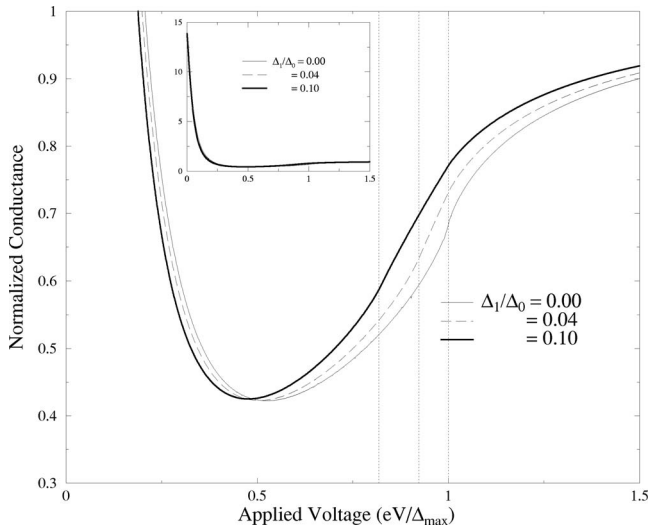

FIG. 4. The conductance curves of {110} junctions for different values of Δ_1. The inset shows the entire conductance curves over the same voltage range. The three dotted vertical lines are plotted at $\Delta_0-\Delta_1$ where $\Delta_1/\Delta_0=0.1$, 0.04, and 0, respectively.

By the same token, the expression for the conductance for c-axis junctions at zero temperature can be obtained as

$$G_{NS}^{c}(V) = \frac{2me^3\Omega}{(2\pi\hbar)^3} V \int d\phi_N \int d\theta_N \sin\theta_N \cos\theta_N [1 + A(V,\phi_N,\theta_N) - B(V,\phi_N,\theta_N)]. \tag{27}$$

In addition to the same parameter set as just mentioned, in the calculation related to c-axis cases, m^* is taken to be m_{ab}^s. The limits of both integrals can be found by comparing the Fermi surfaces of the metal and superconductor.

III. RESULTS AND DISCUSSION

The plots of normalized conductance as a function of applied voltage of all tunneling spectra are shown in Figs. 3–6. The normalized conductance is defined as the conductance divided by its value at infinite applied voltage. Only the tunneling limit is considered. (Z is taken to be 10 in both junction types.) Also, q_F is taken to be equal to $10k_F$ to ensure that all states with positive Fermi velocities of the superconductor are involved in the tunneling process.

For ab-plane junctions, the junction orientations are characterized by α, the angle between the a axis of the superconductor and the interface normal. Three junction orientations, $\alpha=0, \pi/16, \pi/4$, are considered here. Figure 3 shows the conductance plots of $\alpha=0$, or {100} junctions, for different values of Δ_1. The coherence peak around the maximum energy gap grows wider as Δ_1 increases. This peak has edges, where the slope of the conductance changes quite abruptly. The lower energy edge is at $\Delta_0-\Delta_1$ and the higher energy edge is at the maximum gap, $\Delta_{max}=\Delta_0+\Delta_1$. At the latter edge, which appears to be an inflection point of the conductance curve, the slope does not change as suddenly as it does at the former. It should be noted that, although the argument presented in the Introduction regarding the density of states

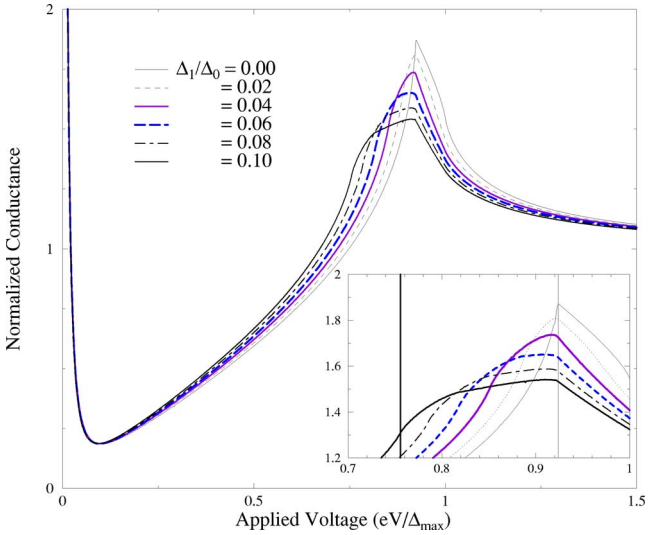

FIG. 5. (Color online) The conductance curves of $\alpha=\pi/16$ junctions for different values of Δ_1. The inset shows the conductance curve around the smaller coherence peak. The vertical lines are plotted at $(\Delta_0\pm\Delta_1)\cos(\pi/8)$ where $\Delta_1/\Delta_0=0.1$ and 0, respectively.

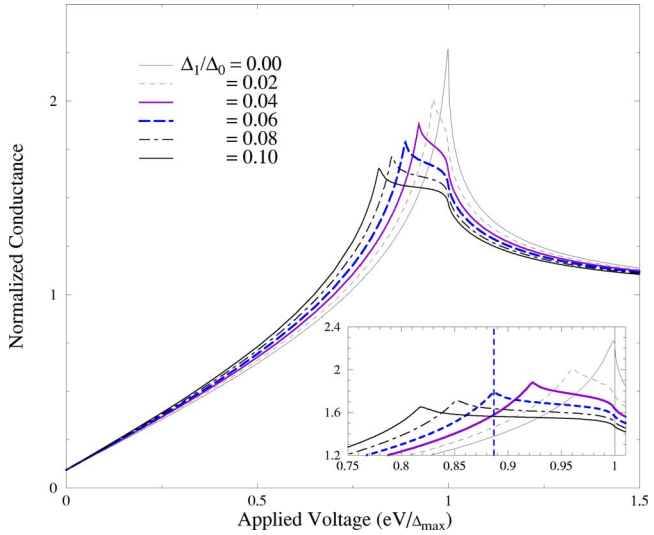

FIG. 6. (Color online) The conductance curves of {001} junctions for different values of Δ_1. The inset shows the detailed conductance curve around maximum gap $\Delta_{max}=\Delta_0+\Delta_1$. The vertical solid line marks the maximum gap and the dotted vertical line indicates $\Delta_0-\Delta_1$, where $\Delta_1=0.06\Delta_0$.

correctly accounts for the positions of these peak edges, it cannot explain why the lower energy edge appears as a kink, while the higher energy edge appears as an inflection point or a smooth curve.

The effect of the k_z variation of the order parameter is not apparent in the conductance spectra of {110}, or $\alpha=\pi/4$, junctions. As can be seen in the inset of Fig. 4, the increase in Δ_1 does not cause dramatic changes in either the width or height of the zero-bias conductance peak. The closer look at the conductance spectra reveals that the height is constant, whereas the width narrows slightly as Δ_1/Δ_0 increases. Also, the inflection point of the spectrum moves inward to $\Delta_0-\Delta_1$. The constant height and the weakly varying width can be understood by considering the following expression for zero-bias conductance peak in the tunneling limit[40]

$$G_{\mathrm{ZBCP}}(eV)=\frac{4e^2}{h}\left\langle\frac{2\Gamma_k^2}{(eV)^2+\Gamma_k^2}\right\rangle_{k_y,k_z}, \tag{28}$$

where the angular brackets denote the average over k_y and k_z, $\Gamma_k=\frac{1}{2}\Delta_k P_k$ where P_k is the transmission probability of the junction when the superconductor is in the normal state. The peak height is equal to $8e^2/h$, obviously independent of Δ_k. As for the width, because the maximum width of $2\Gamma_k^2/[(eV)^2+\Gamma_k^2]$ as a function of eV for each k_z varies from $\frac{1}{2}P_k(\Delta_0-\Delta_1)$ (for $k_z=\pm\pi/c$) to $\frac{1}{2}P_k(\Delta_0+\Delta_1)$ (for $k_z=0$), the value of $\langle 2\Gamma_k^2/[(eV)^2+\Gamma_k^2]\rangle_{k_y}$ for $k_z=0$ would have the largest width and that for $k_z=\pm\pi/c$ would have the smallest width. Thus, the width of zero-bias conductance peak, which is the result of an average over all k_y and k_z, becomes narrower as Δ_1 gets bigger. However, the relative change in this width is only $\Delta_1/\Delta_{max}\ll 1$.

Figure 5 depicts the conductance spectra of $\alpha=\pi/16$ junctions for different values of Δ_1. In addition to the zero-bias conductance peak, another much smaller coherence peak occurs around $(\Delta_0-\Delta_1)\cos 2\alpha$. This value is the magnitude of the order parameter of states with $\vec{k}$ parallel to the interface normal. The increase in Δ_1 affects this peak in the same way as it does the coherence peak in the tunneling spectra of {100} junctions. The sharper edges, where the slopes change sign, are at $\Delta(\phi=0,k_z=0)=(\Delta_0+\Delta_1)\cos(\pi/8)$. There are also inflection points occurring at $|\Delta(\phi=0,k_z=\pm\pi/c)|=(\Delta_0-\Delta_1)\cos(\pi/8)$.

Figure 6 shows the conductance plots of {001} junctions, for different values of Δ_1. Similar to {100} junctions, the coherence peak around the maximum energy gap becomes wider as Δ_1 gets bigger. The slope of the conductance changes abruptly from being positive to negative at $\Delta_0-\Delta_1$. The other edge, which is an inflection point, occurs at the maximum gap. It should be noted for {001} junctions the abrupt change in slope of the conductance curve at $\Delta_0-\Delta_1$ causes a sharper peak than in the spectra of {100} junctions.

In summary, the c-axis variation of $d_{a^2-b^2}$-wave does not affect zero-bias conductance peak but it causes the widening of the coherence peak of the conductance spectra. The width of the peak is proportional to the magnitude of the c-axis pairing order parameter. These results suggest that the width of the coherence peak of tunneling conductance of $d_{a^2-b^2}$-wave superconductors can be used as a measurement of the strength of the interlayer pairing interaction. The widening of the coherence peak has been seen in $Bi_2Sr_2CaCu_2O_{8+\delta}$ and $YBa_2Cu_3O_7$ (see, for example, Refs. 41 and 42). From a rough estimation of the width of the coherence peak (see note[43]), Δ_1 of optimally doped $Bi_2Sr_2CaCu_2O_{8+\delta}$ is around 5 meV, or $\Delta_1=0.13\Delta_0$ (from data in Ref. 41), and Δ_1 of $YBa_2Cu_3O_7$ is around 7 meV, or $\Delta_1=0.18\Delta_0$ (from data in Ref. 42). It should be noted that because $Bi_2Sr_2CaCu_2O_{8+\delta}$ is a bilayer material, the widening of this peak may be due to the bilayer splitting. As mentioned earlier, the bilayer splitting can cause the splitting of the coherence peak and the size of the splitting depends on

the strength of the bilayer interaction.[28] Therefore, if the splitting is smaller than the experimental resolution of the conductance spectrum, the coherence peak may appear to be broadened instead of appearing as two peaks. In order to distinguish whether the observed width is due to the *c*-axis variation or the bilayer splitting, the energy resolution of the measurement must be much smaller than the splitting.

Although a continuous model was employed here, it is expected that the main qualitative results will also be valid for a discrete model. For instance, as shown in Ref. 22, for junctions with orientation away from {100} and {110}, in addition to a coherence peak at the magnitude of the energy gap along the interface normal vector and a ZBCP, there exists another peak at the magnitude of the energy gap at the edge of the surface-adapted Brillouin zone. This peak will be affected by the k_z variation of the energy gap in the same way as is the coherence peak and the peak at the magnitude of the energy gap along the interface normal.

IV. CONCLUSION

This article is a theoretical study of the effect of *c*-axis variation of $d_{a^2-b^2}$-wave order parameter, i.e., of finite interlayer pairing, on tunneling spectroscopy of normal metal-layered superconductor junctions. The *c*-axis variation of the order parameter has been found to have an insignificant effect on the zero-bias conductance peak. The height of the zero-bias conductance peak in fact does not change with the degree of the variation. The width decreases when the interlayer pairing order parameter gets stronger. However, this decrease is very small. This small effect on the width of the zero-bias conductance peak is not surprising. It was shown that the width is also unaffected by the presence of impurities and surface roughness.[44]

The *c*-axis variation of the order parameter has much larger effect on the coherence peak in the tunneling spectrum. The variation of the order parameter causes the widening of coherence peak. It is found that the width of the peak is proportional to the interlayer pairing order parameter, Δ_1. The results indicate the conductance spectra, which contain coherence peaks, can be used to detect the *c*-axis variation of the order parameter.

ACKNOWLEDGMENTS

I would like to thank M. B. Walker and M. F. Smith for their useful comments and discussions. This work is financially supported by Thailand Toray Science Foundation (TTSF).

*Electronic address: pairor@sut.ac.th

[1] E. L. Wolf, *Principles of Electron Tunneling Spectroscopy* (Oxford University Press, New York, 1989).
[2] W. L. McMillan and J. M. Rowell, in *Superconductivity*, edited by R. D. Parks (Marcel-Dekker, New York, 1969), Vol. 1, p. 561.
[3] M. Tinkham, *Introduction to Superconductivity* (McGraw-Hill, New York, 1996).
[4] C.-R. Hu, Phys. Rev. Lett. **72**, 1526 (1994).
[5] J. Yang and C.-R. Hu, Phys. Rev. B **50**, 16766 (1994).
[6] S. Kashiwaya, Y. Tanaka, M. Koyanagi, and K. Kajimura, Phys. Rev. B **53**, 2667 (1996).
[7] Y. Tanaka and S. Kashiwaya, Phys. Rev. Lett. **74**, 3451 (1995).
[8] C.-R. Hu, Phys. Rev. B **57**, 1266 (1998).
[9] M. C. Gallagher, J. G. Adler, J. Jung, and J. P. Franck, Phys. Rev. B **37**, 7846 (1988).
[10] J. Geerk, X. X. Xi, and G. Linker, Z. Phys. B: Condens. Matter **73**, 329 (1988).
[11] D. Mandrus, L. Forro, D. Koller, and L. Mihaly, Nature (London) **351**, 460 (1991).
[12] T. Walsh, J. Moreland, R. H. Ono, and T. S. Kalkur, Phys. Rev. Lett. **66**, 516 (1991).
[13] J. Lesueur, L. H. Greene, W. L. Feldman, and A. Inam, Physica C **191**, 325 (1992).
[14] A. M. Cucolo and R. Di Leo, Phys. Rev. B **47**, 2916 (1993).
[15] S. Kashiwaya, Y. Tanaka, M. Koyanagi, H. Takashima, and K. Kajimura, Phys. Rev. B **51**, 1350 (1995).
[16] L. Alff, H. Takashima, S. Kashiwaya, N. Terada, H. Ihara, Y. Tanaka, M. Koyanagi, and K. Kajimura, Phys. Rev. B **55**, R14757 (1997).
[17] S. Sinha and K.-W. Ng, Phys. Rev. Lett. **80**, 1296 (1998).
[18] J. Y. T. Wei, N.-C. Yeh, D. F. Garrigus, and M. Strasik, Phys. Rev. Lett. **81**, 2542 (1998).
[19] J. Y. T. Wei, C. C. Tsuei, P. J. M. van Bentum, Q. Xiong, C. W. Chu, and M. K. Wu, Phys. Rev. B **57**, 3650 (1998).
[20] I. Iguchi, W. Wang, M. Yamazaki, Y. Tanaka, and S. Kashiwaya, Phys. Rev. B **62**, R6131 (2000).
[21] H. Aubin, L. H. Greene, Sha Jian, and D. G. Hinks, Phys. Rev. Lett. **89**, 177001 (2002).
[22] P. Pairor and M. B. Walker, Phys. Rev. B **65**, 064507 (2002).
[23] P. Pairor and M. F. Smith, J. Phys.: Condens. Matter **15**, 4457 (2003).
[24] W. Kim and J. P. Carbotte, Phys. Rev. B **63**, 054526 (2001).
[25] W.-C. Wu, Phys. Rev. B **65**, 052508 (2002).
[26] S. E. Barnes and S. Maekawa, Phys. Rev. B **67**, 224513 (2003).
[27] B. W. Hoogenboom, C. Berthod, M. Peter, Ø. Fischer, and A. A. Kordyuk, Phys. Rev. B **67**, 224502 (2003).
[28] Y. H. Su, J. Chang, H. T. Lu, H. G. Luo, and T. Xiang, Phys. Rev. B **68**, 212501 (2003).
[29] A. Bansil, M. Lindroos, S. Sahrakorpi, and R. S. Markiewicz, Phys. Rev. B **71**, 012503 (2005).
[30] A. K. Rajagopal and S. S. Jha, Phys. Rev. B **54**, 4331 (1996).
[31] S. S. Jha and A. K. Rajagopal, Phys. Rev. B **55**, 15248 (1997).
[32] M. B. Walker (unpublished).
[33] G. H. Wannier, *Elements of Solid State Theory* (Cambridge University Press, London, 1959).
[34] A. Griffin and J. Demers, Phys. Rev. B **4**, 2202 (1971).
[35] G. E. Blonder, M. Tinkham, and T. M. Klapwijk, Phys. Rev. B **25**, 4515 (1982).
[36] B. Jannossy, R. Hergt, and L. Fruchter, Physica C **170**, 22 (1990).

[37] T. R. Chien, W. R. Datars, M. D. Lan, J. Z. Liu, and R. N. Shelton, Phys. Rev. B **49**, 1342 (1994).
[38] C. P. Poole, H. A. Farach, and R. J. Creswick, *Superconductivity* (Academic Press, New York, 1995), p. 154.
[39] N. P. Ong, O. K. C. Tsui, K. Krishana, J. M. Harris, and J. B. Peterson, Chin. J. Phys. (Taipei) **34**, 432 (1996).
[40] M. B. Walker and P. Pairor, Phys. Rev. B **59**, 1421 (1999).
[41] Ch. Renner, B. Revaz, J.-Y. Genoud, K. Kadowaki, and Ø. Fischer, Phys. Rev. Lett. **80**, 149 (1998).
[42] T. Cren, D. Roditchev, W. Sacks, and J. Klein, Europhys. Lett. **52**, 203 (2000).
[43] The width of the coherence peak of the conductance spectrum is estimated by measuring the energy difference between the two points within the coherence peak where the slope changes abruptly, or sharp edges appear.
[44] M. B. Walker and P. Pairor, Phys. Rev. B **60**, 10395 (1999).